Eur. Phys. J. B **41**, 439–444 (2004)
DOI: 10.1140/epjb/e2004-00336-1

THE EUROPEAN PHYSICAL JOURNAL B

Nucleation of superconductivity in finite metallic multilayers: Effect of the symmetry

V.N. Kushnir[1], S.L. Prischepa[1,2], C. Cirillo[2], M.L. Della Rocca[2], A. Angrisani Armenio[2], L. Maritato[3], M. Salvato[2], and C. Attanasio[2,a]

[1] Belarus State University of Informatics and Radioelectronics, P. Browka str. 6, Minsk 220013, Belarus
[2] Dipartimento di Fisica "E.R. Caianiello" and INFM-Laboratorio Regionale Supermat, Università degli Studi di Salerno, 84081 Baronissi (SA), Italy
[3] Dipartimento di Fisica "E.R. Caianiello" and INFM-Coherentia, Università degli Studi di Salerno, 84081 Baronissi (SA), Italy

Received 3 December 2003 / Received in final form 23 July 2004
Published online 5 November 2004 –

Abstract. The influence of the finite dimensions of superconducting metallic multilayers on H-T phase diagram is studied. It is established that the geometrical symmetry of the samples determines crucially the $H_{c2||}(T)$ dependencies. For samples where the symmetry plane is in the middle of the superconducting layer the $H_{c2||}$ values are, for temperatures close to T_c, larger than the $H_{c2||}$ values of the samples for which the symmetry plane lies in the middle of the normal layer. The results are analysed on the basis of the Ginzburg-Landau approach and are explained by considering the different symmetry of the wave function describing the system. The experimental results are in good agreement with the elaborated model, which takes into account the actual symmetry of the samples.

PACS. 74.78.Fk Multilayers, superlattices, heterostructures – 74.20.De Phenomenological theories (two-fluid, Ginzburg-Landau, etc.) – 74.45.+c Proximity effects; Andreev effect; SN and SNS junctions

1 Introduction

Superconductor/normal metal (S/N) multilayers are still very effective structures to study the effects of proximity [1], periodicity and a-periodicity [2,3], finite dimensions [4], surfaces of the sample [5] on the superconducting phase transitions [6] as well as on the vortex properties [7,8]. In particular the behaviour of the upper critical field H_{c2} as function of temperature T is a probe of the strength and of the nature of the coupling between the S layers [2,9]. The investigation of peculiarities in $H_{c2}(T)$ (i.e. positive curvature, no evidence of saturation at low temperatures) gives a better understanding of the mechanisms of superconductivity in such structures [10].

When the magnetic field is oriented in the direction parallel to the layers, the thermodynamic properties of S/N multilayers are closely related to the spatial behaviour of the order parameter. When a multilayer consists of a stack of thin superconducting films, in which the amplitude of the order parameter is almost constant (this is the criterion of bi-dimensionality (2D) of thin film), separated by films of nonsuperconducting metals, the total dimensionality of the multilayer depends on the relation between the period of the multilayer Λ (which is constant) and the superconducting coherence length in the perpendicular direction $\xi_\perp$ (which is a temperature dependent parameter, $\xi_\perp(T) \sim (1 - T/T_c)^{1/2})$ having the physical meaning of the characteristic dimension on which the order parameter changes significantly. When $\xi_\perp(T)$ is larger than Λ, the multilayer behaves like a three-dimensional (3D) system and the temperature dependence of the parallel critical magnetic field, assuming the well-working Ginzburg-Landau approach, is linear, $H_{c2||} = \Phi_0/2\pi\xi_\perp\xi_{||} \sim (T_c - T)$. When $\xi_\perp(T)$ is less than Λ, the system is bi-dimensional and $H_{c2||} = \Phi_0/2\pi\Lambda\ \xi_{||} \sim (T_c - T)^{1/2}$. Here $\xi_{||}$ is the superconducting coherence length in the parallel direction. Such temperature dependent crossover in system dimensionality was observed in different S/N multilayers [8,11–14].

The background for the microscopic theoretical investigation of S/N multilayers close to H_{c2} was given by Takahashi and Tachiki (TT) [2]. Even if this theory nicely describes the main features of the H-T phase diagram of metallic multilayers (i.e. the anisotropy value, the presence of dimensional crossover), it is not able to fit quantitatively the experimental data [15]. In fact it was developed for the case of infinite superlattice and boundary effects (in particular, surface superconductivity) were not taken into account. Nevertheless it is known that surface nucleation of the order parameter can significantly influences the H-T plot [16–18]. Until now there are no exhaustive experimental investigations of the nucleation of superconductivity in periodic multilayers especially taking into account

[a] e-mail: attanasio@sa.infn.it

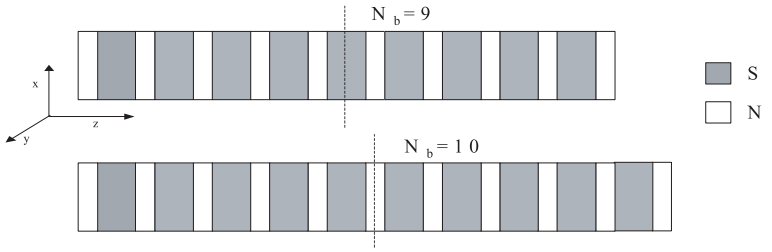

Fig. 1. The geometrical configuration of the Nb/Pd samples for $N_b = 9$ and $N_b = 10$.

the possible strong influence of the sample edges [4,6,19]. Metallic S/N multilayers are very good model object for such kind of study because it exists a rather high comprehension of the proximity effect in them [20–22].

In this article we present the results of the investigation of the nucleation of superconductivity when the magnetic field is applied in the parallel direction for different S/N systems and for different (odd and even) number of bilayers, N_b. Nb/Pd and Nb/Cu samples have been chosen.

The choice of Nb for fabrication of the superconducting multilayers was related to its highest critical temperature among the single superconducting elements. The choice of Cu was related to the possibility of creating the Nb/Cu multilayers with high quality structural properties [23]. Moreover the proximity effect is very well studied in this system [9,11]. On the other hand, we choose Pd because among the normal metals it turns out to be particularly interesting. It is in fact characterized by a large value of the spin susceptibility and in some alloys (i.e. $Pd_{1-x}Co_x$, $Pd_{1-x}Fe_x$) shows a ferromagnetic behavior even for small values of x [24]. Moreover, the interface of Nb/Pd system is more transparent with respect to Nb/Cu one [25]. These differences between two studied systems give us the good opportunity to generalize the observed symmetry effect to the class of the proximity coupled metallic multilayers.

For all the samples the top and the bottom layers are made with the normal metal. So, taking into account the constant period of the multilayer, the central layer is superconducting in the case of odd N_b and normal for even N_b. This means that for odd (even) N_b values, plus the capping N layer, the symmetry plane of the whole sample falls in the centre of the S(N) layer (see Fig. 1).

The thickness of S layers d_S is always 200 Å for both compositions. In Nb/Pd samples, the Pd thickness d_N is equal to 100 Å. In fact, as recently shown, 100 Å of Pd reveals the presence of the temperature induced dimensional crossover in Nb/Pd systems [14]. When such thickness increases towards 200 Å, the system behaves as 2D in the whole temperature range [14]. For Nb/Cu system we chose $d_N = d_S = 200$ Å. In fact, for these values a pronounced 2D-3D crossover is usually observed at the crossover temperature T^* [9,11]. We show that changing the number of bilayers N_b, i.e. changing the symmetry of the samples, a drastic change in the dimensionality of the system at $T \to T_c$ occurs, with a 2D behaviour almost up to T_c for samples in which the symmetry plane lies in the centre of the S layer.

2 Experimental

Pairs of Nb/Pd and Nb/Cu samples with 9 and 10 total number of N_b were grown on Si(100) substrates at room temperature by using a dual source magnetically enhanced *dc* triode sputtering system [6,14]. The deposition rates were 9 Å/s for Nb, 8 Å/s for Pd and 5 Å/s for Cu. Nb/Cu samples were deposited in different deposition runs, while Nb/Pd samples were sputtered simultaneously. A specially designed movable shutter allowed the simultaneous deposition of the two samples with different number of bilayers. The starting position of the sample holder was located between the Pd and Nb guns and two substrates were mounted on it. $N_b + 1$ bilayers were deposited on the substrate positioned closest to the Pd target, while N_b bilayers were deposited on the other substrate. The platform where the samples are mounted can rotate, using a step motor, in a controlled way over 360 degrees to reach every position. At the beginning of the process the sample holder is sent to the Pd gun to sputter the first layer (the two samples will consist of N_b or $N_b + 1$ Nb/Pd bilayers plus a bottom Pd layer). Then, after Pd deposition, the sample holder is moved, through the zero position, to the Nb gun. This movement (from the Nb to the Pd gun) is repeated alternatively until on both samples N_b bilayers plus the Pd bottom layer have been sputtered. The sample holder is moved now from the Pd to the Nb gun in the direction opposite to the zero position to sputter the Nb layer only on one sample. The sample holder has a diameter of 2.5 cm and the distance between the two substrates is almost 2 cm and this allows us to use a screen, close the Nb gun, to prevent Nb deposition also on another sample during this last Nb deposition. After this, the sample holder is slightly moved back and the Nb gun is switched off. When we are sure that the Nb rate is zero (usual waiting time is 1 minute), the sample holder is moved, through the Nb gun, to the zero position and finally to the Pd gun to sputter the last Pd layer only on this second sample. This last step is possible due to the presence of another screen close the Pd gun. Finally the sample holder is moved back to the zero position and the deposition is over.

X-ray reflectivity measurements confirmed the layered structure of the samples with the interface roughness order of 10 Å [14]. Transport measurements with a standard four probe technique were performed for both parallel and perpendicular magnetic field orientations. The resistance was measured with the accuracy of 10^{-4} ohm, while the measured accuracy of magnetic field was 10^{-4} T.

Table 1. Parameters of the investigated samples.

Sample	N_b	d_S (Å)	d_N (Å)	T_c (K)	β_{10}	ρ_{10} ($\mu\Omega$·cm)	$\xi_{\|\|}(0)$ (Å)	P	ξ_{NC} (Å)	ξ_{S0} (Å)
SP	9	200	100	3.68	1.6	9.5	127	0.4	52	103
NP	10	200	100	4.22	1.6	9.5	125	0.4	48	96
SC	9	200	200	6.23	1.6	8.4	116	0.27	74	116
NC	10	200	200	6.67	1.6	8.4	120	0.27	74	117

The samples from each pair were simultaneously mounted in an insert with the possibility to rotate them in the liquid helium bath. A superconducting Nb-Ti solenoid with $T_c = 7.2$ K was used to produce the external magnetic field. The H_{c2} values were extracted from the $R(T,H)$ curves using the 90% R_N criterion, where R_N is the normal state resistance of the sample just above the transition to the superconducting state. The transition widths ΔT_c in zero field were always less than 20 mK, while at parallel fields higher than 2 tesla their values were less than 300 mK, confirming the high quality of the samples. From $H_{c2\perp}(T)$ curves we have calculated [21] the values of $\xi_{||}(0)$ reported in Table 1. We named the samples using the letter S or N according to whether the symmetry plane lies in the centre of S or in the centre of N layers respectively, followed by a letter that indicates the normal metal used (P for Palladium and C for Copper). For example, SP is the Nb/Pd multilayer whose symmetry plane lies in the S layer ($N_b = 9$) while NC is the Nb/Cu sample with the symmetry plane in the centre of the N layer ($N_b = 10$).

The deposition of the Nb/Pd multilayers in the same run allows us to consider the same Nb as well as the same interface properties in each sample [6,14]. This hypothesis is confirmed by the same resistivity ρ_{10}, the same residual resistivity ratio β_{10} and the same $\xi_{||}(0)$ values for these two samples. The macroscopic parameters of Nb/Cu samples were also very similar. So we believe that the only difference between each pair of samples is in their symmetry due to their different finite dimensions.

The choice of 9 and 10 number of bilayers for samples studied in this work was based on the result of our previous research [6]. In reference [6] the effect of symmetry on the resistive characteristics of Nb/Cu multilayers prepared in the same way as in this work was investigated for N_b in the range 5...12. It was shown, for $N_b > 10$ the symmetry effect becomes less pronounced due to the smaller influence of the surface effects with increasing the N_b value. In order to demonstrate the validity of the observed phenomena we have also prepared another pair of Nb/Cu samples with N_b equal to 5 and 6 and $d_N = d_S = 200$ Å. Again this couple of multilayers have been fabricated in the same deposition run.

In Figure 2a we present the measured temperature dependencies of parallel and perpendicular magnetic fields for the sample NP. The behaviour of $H_{c2||}(T)$ reveals the conventional 2D-3D crossover for S/N multilayers [2–4,8,9,12–14].

In Figure 2b we present the H-T phase diagram for sample SP, with the symmetry plane in the centre of the Nb layer. As it is clearly seen, while the $H_{c2\perp}(T)$ dependence is very similar to that of NP sample, the $H_{c2||}(T)$ curve is quite different. We did not see the pronounced linear part in the $H_{c2||}(T)$ dependence as it is usually observed for S/N multilayers in the case of $d_N \approx d_S \approx \xi_S$. The $H_{c2||}(T)$ curve seems to be square root like in the whole temperature range, even close to T_c, which is the signature of the 2D behaviour.

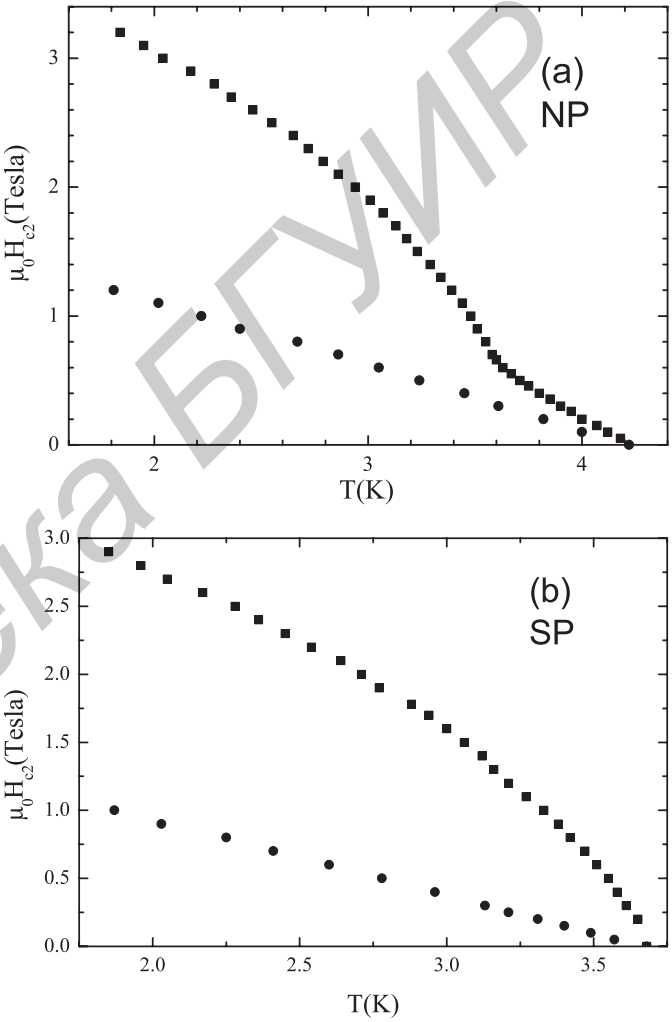

Fig. 2. (a) H-T phase diagram for the sample NP. Squares (circles) refer to $H_{c2||}$ ($H_{c2\perp}$). (b) H-T phase diagram for sample SP. Squares (circles) refer to $H_{c2||}$ ($H_{c2\perp}$).

As already pointed out, both the samples SP and NP were obtained in the same deposition run, and present the same Nb properties and Nb/Pd interface behaviours. The only difference between these two samples is the different

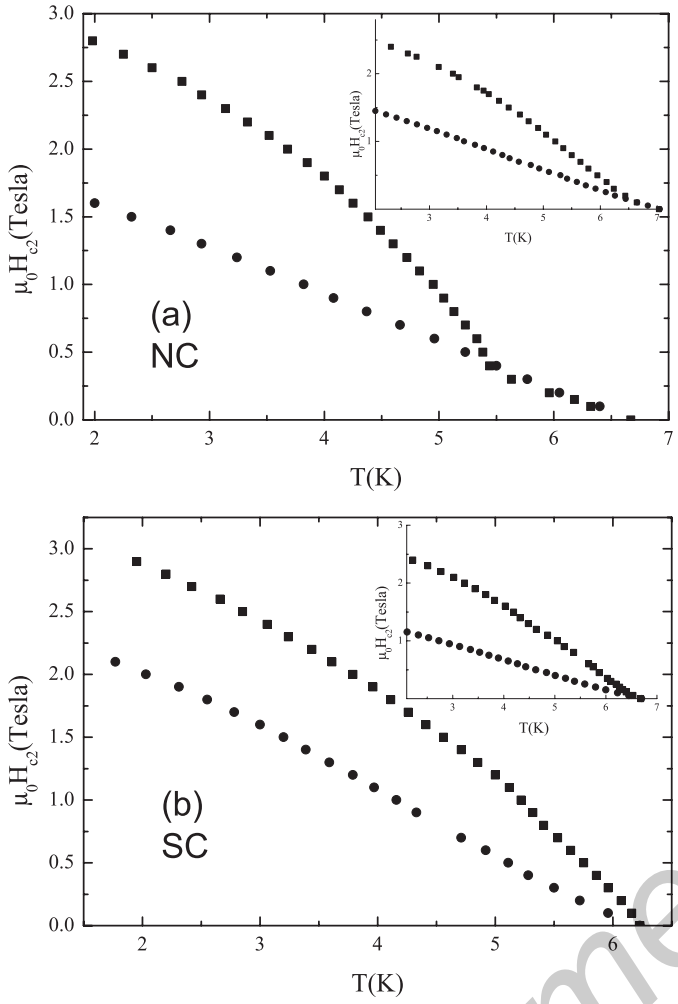

Fig. 3. (a) H-T phase diagram for sample NC. Squares (circles) refer to $H_{c2||}$ ($H_{c2\perp}$). Inset: the same for sample Nb/Cu with $N_b = 6$. (b) H-T phase diagram for sample SC. Squares (circles) refer to $H_{c2||}(H_{c2\perp})$. Inset: the same for sample Nb/Cu with $N_b = 5$.

number of bilayers and, consequently, their different symmetry. To confirm the effect of the samples' symmetry on the $H_{c2||}(T)$ dependencies we have investigated another S/N system. We have fabricated and measured a pair of multilayers with a different N material, namely Nb/Cu, with 10 (NC sample) and 9 (SC sample) bilayers. Taking into account the absence of the large spin susceptibility in Cu with respect to Pd [24], the thickness of Cu was larger, $d_{\rm N} = 200$ Å. The results of the $H_{c2}(T)$ measurements for NC and SC samples are presented in Figures 3a and 3b respectively. Again the $H_{c2||}(T)$ dependence for the sample NC is usual for S/N multilayers, revealing a pronounced 3D-2D crossover, and the $H_{c2||}(T)$ dependence for the sample SC is square root like in the whole temperature range up to T_c. In the inset to Figure 3a we show the H-T plot for Nb/Cu multilayer with $N_b = 6$ and in the inset to Figure 3b H-T phase diagram is presented for another Nb/Cu sample with $N_b = 5$. Also in this case the behavior of $H_{c2||}$ versus T depends almost only on the symmetry of multilayers. Based on the obtained results for different systems and for different number of bilayers, we may conclude that the observed increasing of the temperature interval of the 2D nature of samples with the symmetry plane in the centre of S layer is a general feature of S/N metallic multilayers. According to our opinion, this behaviour is mainly due to the effect of finite dimensions on the nucleation of superconductivity. In order to get deeper insight in the problem, we elaborated a model of superconductivity nucleation in the presence of free surfaces for S/N multilayers.

3 Model

Our description will assume two layered systems with identical properties except for the total number of bilayers. For qualitative analysis of the superconducting phase in the vicinity of the parallel critical magnetic field we will follow the standard procedure, applying the appropriate boundary conditions [2,20] to the Ginzburg-Landau (GL) equation for the order parameter $\Psi(r)$:

$$-\left(\nabla - i\frac{2\pi}{\Phi_0}A(r)\right)^2 \Psi(r) = \varepsilon(z;T)\Psi(r), \qquad (1)$$

where Φ_0 is the flux quantum, $A(r)$ is the vector potential which we take in the form $A = (Hz,\ 0,\ 0)$ and $\varepsilon(z;T)$ is a step function coefficient, which we chose in the form [19]

$$\varepsilon(z;T) = \begin{cases} \dfrac{2\pi H_{\rm S0}}{\Phi_0}\cdot\left(1-\dfrac{T}{T_S}\right), & z \in I_{\rm S} \\ \dfrac{2\pi H_{\rm NC}}{\Phi_0}\cdot\dfrac{T}{T_c}, & z \in I_{\rm N} \end{cases}$$

where $I_{\rm S}$ and $I_{\rm N}$ are the intervals of z values corresponding to S and N layers respectively, $H_{\rm S0(NC)}$ are the superconducting parameters in the S(N) layer at zero critical temperature ($H_{\rm S0(NC)} = \Phi_0/2\pi\xi^2_{\rm S0(NC)}$, $\xi_{\rm S0(NC)}$ being the coherence length in S(N) layer respectively), T_S is the critical temperature of the superconducting slab. In the following the coordinate system has the XY plane parallel to the layer surfaces, coinciding with the symmetry plane of the S/N structure, and the Z axis perpendicular to the surface of the layers, as shown in Figure 1. The external magnetic field H is directed along the Y axis. Separating the variables in equation (1), that is writing $\Psi(r) = e^{ikx}\psi(z)$, we obtain the following equation:

$$\left\{\frac{\partial^2}{\partial z^2} + \varepsilon(z;T) - \frac{1}{\varsigma_H^4}(z-z_0)^2\right\}\psi(z) = 0, \qquad (2)$$

where $\zeta_H^2 \equiv \Phi_0/2\pi H$ and $z_0 \equiv k\cdot\zeta_H^2$.

The boundary conditions are the following:

$$\left.\frac{\partial\psi}{\partial z}\right|_{-L/2} = \left.\frac{\partial\psi}{\partial z}\right|_{+L/2} = 0, \qquad (3)$$

at the edges of the multilayer (L is the multilayer overall thickness), and

$$\frac{1}{\psi_{\rm S}}\frac{\partial\psi_{\rm S}}{\partial z}\bigg|_{\rm S} = P\frac{1}{\psi_{\rm N}}\frac{\partial\psi_{\rm N}}{\partial z}\bigg|_{\rm N} \qquad (4)$$

at the S/N interfaces (P is the interface transparent coefficient) [20].

Note, that the boundary task (2–4) is formulated in the same manner as in the simplest one mode approach of the microscopic theory [2]. And the chosen temperature dependence of the coefficient function $\varepsilon(z;T)$ could be considered as linear interpolation of the true temperature dependence. We wish to point out that the used simplification is not substantially from the viewpoint of the considered problem.

Solutions to equations (2–4) have been found using for each z_0 a standard procedure based on the sequential joining of solutions in N and S layers by applying each time equation (4). The maximum value of the external magnetic field parameter H_{max} for which condition (3) is satisfied is the upper critical field. Assigning a performing GL functional to equation (1) we can calculate in self-consistent manner the z_0 parameter from the variational principle, which gives

$$z_0 = \frac{\int z\psi^2(z;z_0)dz}{\int \psi^2(z;z_0)dz}. \qquad (5)$$

In the case of an infinite superlattice, the presence of an infinite number of XY symmetry planes produces a degeneracy in the z_0 parameter, $H_{max}(z_0+\Lambda) = H_{max}(z_0)$ (Λ being the period of multilayer, $\Lambda = d_{\rm N}+d_{\rm S}$). As shown in reference [19], this maximum value of H_{max} is obtained when z_0 falls in the centre of any S layer.

In the case of a finite layered system, at least at temperatures close to T_c, where the wave function smears over the whole sample, it is essential to take into account the finite dimensions of the structure. The system will present now only a single symmetry plane, situated in the centre of a S layer (samples SP, SC) or of a N layer samples (NP, NC). That is why equation (5) always has the solution $z_0 = 0$, which corresponds to the symmetric functions $\psi(z)$. At $T = T_{\rm c}$ this solution is unique for both kinds of the samples. At lower temperatures, for samples with the symmetry plane in the centre of S layer it is still $z_0 = 0$, while for another samples (symmetry plane is in the centre of N layer) z_0 is temperature dependent and reaches the value $\pm\Lambda/2$ at low temperatures.

To fit the experimental $H_{c2||}(T)$ dependencies we solve equations (2–4), for samples SP and SC, with $z_0 = 0$. For samples NP and NC the same procedure has been applied for $z_0 = 0$ (symmetrical solution) and $z_0 = \pm\Lambda/2$. We got, that the $H_{c2||}(T)$ dependence in the temperature region $T \in (T^*,\ T_c)$ corresponds to the state with the symmetry function $\psi(z)$, i.e. to $z_0 = 0$; when lowering the temperature from T^* the z_0 values change abruptly from $z_0 = 0$ to $z_0 = \pm\Lambda/2$. The results of these calculations are presented in Figure 4a (for SP and NP samples) and in Figure 4b (for SC and NC samples) by drawn lines. The

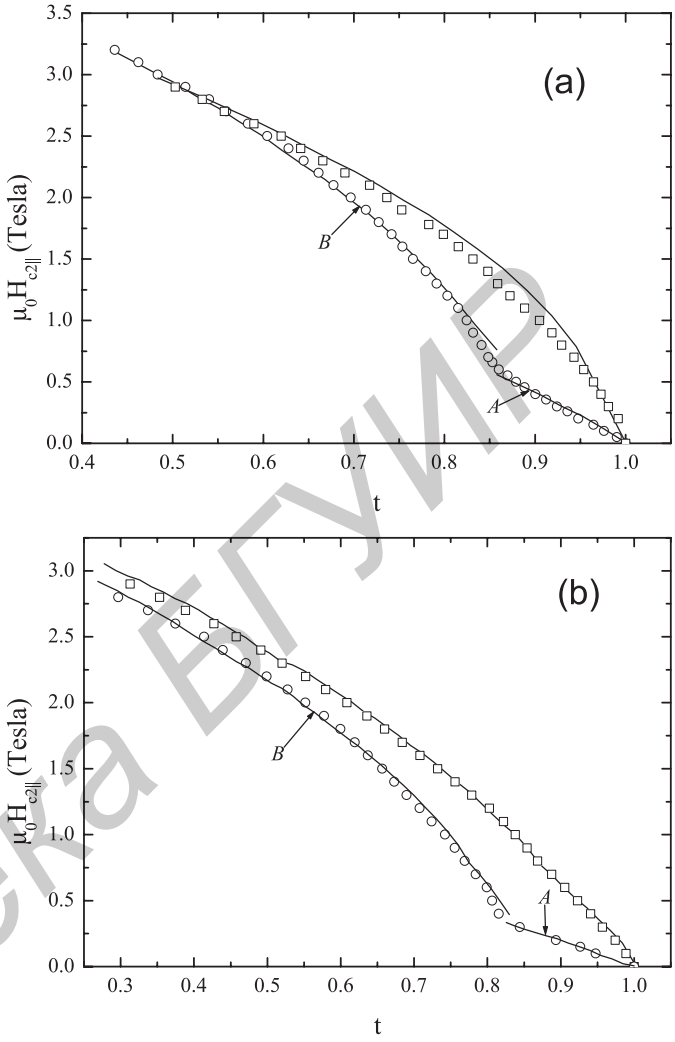

Fig. 4. (a) Parallel magnetic fields for samples SP (squares) and NP (circles) versus the reduced temperature t together with the results of the fitting procedure (lines) according to equations (2–5). (b) Parallel magnetic fields for sample SC (squares) and NC (circles) versus reduced temperature t together with the results of the fitting procedure (lines) according to the equations (2–5). The parts of the theoretical curves for NP and NC samples labelled by letters A and B are related to the $z_0 = 0$ and $z_0 = \pm\Lambda/2$ values, respectively (see text).

agreement with the experimental data is satisfactory. The theoretical curves reasonably describes the main features of the H-T plot. The fitting parameters, P, $\xi_{\rm NC}$ and $\xi_{\rm S0}$, are reported in Table 1.

In the zero temperature limit (or at large values of the magnetic field) the $H_{c2||}(T)$ curves calculated for the NP and NC samples tend to those obtained for the SP and SC samples respectively. This is exactly what expected in the proposed model when the wave function is localized within a single S layer [2]. In fact, in this case the sample is practically equivalent to an infinite multilayer (the sample boundaries do not appreciably influence the behaviour of the overall system) and the infinite structure

symmetry is *re-established* in the multilayer. To observe this effect on $H_{c2||}(T)$ curves a crucial role is played by the symmetry of the samples. The geometrical symmetry plane has to be exactly in the centre of the middle S or N layers, otherwise the symmetry effect of the GL wave function at $T \to T_c$ will be ruined and the effect will not be observed.

4 Conclusion

In conclusion, investigations of the influence of the finite dimensions of the S/N proximity coupled multilayers on the superconducting phase nucleation have been performed. Experiments were done on two different systems, Nb/Pd and Nb/Cu, with different relation between d_S and d_N. In the case of Nb/Pd pair of samples, with $d_N = d_S/2 = 100$ Å and with different number of bilayers (9 and 10) was deposited in the same deposition run. Pair of Nb/Cu multilayers also with $N_b = 9$ and $N_b = 10$ and $d_N = d_S = 200$ Å was deposited in different deposition runs, but the main physical parameters of the samples were also very similar. Moreover, a pair of Nb/Cu samples with $N_b = 5$ and $N_b = 6$ was also deposited simultaneously in order to check the influence of number of bilayers on the effect of symmetry. The observed $H_{c2||}(T)$ dependences were different in the two cases. For samples with the symmetry plane situated in the middle of N layer the $H_{c2||}(T)$ curves are typical for S/N multilayers, presenting the well known 3D-2D crossover at a certain $T^* < T_c$. For samples with the symmetry plane in the middle of S layer the $H_{c2||}$ values are much higher in the region $T \to T_c$, revealing an almost 2D behaviour up to the critical temperature. The difference has been explained in terms of the change of the symmetry of the GL wave function describing the system. Namely, it changes from the infinite superlattice symmetry for large values of the applied magnetic field to the symmetry of the real structure for small values of the field (or for $T \to T_c$). In the last case the superconducting nucleus is only one for the sample with the symmetry plane in the S layer and it appears in the central S layer. For the sample with the symmetry plane in the N layer the number of superconducting nuclei are two and they appear in the S layers right above and below the central N layer. Consequently, in the second case the $H_{c2||}$ values are smaller. The obtained results addresses possible important inaccuracies in the description of a layered system as an infinite superlattice and points out the importance of considering the actual symmetry of the system when analysing the H-T phase diagram of finite superconducting multilayers.

References

1. P.M. Ostrovsky, M.A. Skvortsov, M.V. Feigel'man, JETP **96**, 355 (2003); C. Chiuhu, A. Lodder, Phys. Rev. B **64**, 224526 (2001)
2. S. Takahashi, M. Tachiki, Phys. Rev. B **33**, 4620 (1986)
3. A. Sidorenko, C. Sürgers, T. Trappmann, H.V. Löhneysen, Phys. Rev. B **53**, 11751 (1996); M.G. Karkut, J.-M. Triscone, D. Ariosa, Ø. Fischer, Phys. Rev. B **34**, 4390 (1986)
4. C. Chiuhu, A. Lodder, Superlatt. Microstruc. **30**, 95 (2001)
5. H.J. Fink, S.B. Haley, `cond-matt/0303121` (unpublished)
6. V.N. Kushnir, S.L. Prischepa, M.L. Della Rocca, M. Salvato, C. Attanasio, Phys. Rev. B **68**, 212505 (2003)
7. S.H. Brongersma, E. Verweij, N.J. Koeman, D.G. de Groot, R. Griessen, B.I. Ivlev, Phys. Rev. Lett. **71**, 2319 (1993)
8. C. Coccorese, C. Attanasio, L.V. Mercaldo, M. Salvato, L. Maritato, J.M. Slaughter, C.M. Falco, S.L. Prischepa, B.I. Ivlev, Phys. Rev. B **57**, 7922 (1998)
9. R.A. Klemm, A. Luther, M.R. Beasley, Phys. Rev. B **12**, 877 (1975); C.S.L. Chun, G.-G. Zheng, J.L. Vicent, I.K. Schuller, Phys. Rev. B **29**, 4915 (1984); K.R. Biagi, V.G. Kogan, J.R. Clem, Phys. Rev. B **32**, 7165 (1985)
10. V.N. Zavaritsky, V.V. Kabanov, A.S. Alexandrov, Europhys. Lett. **60**, 127 (2002); E.S. Caixeiro, J.L. González, E.V.L. de Mello, Phys. Rev. B. **69**, 024521 (2004)
11. I. Banerjee, I.K. Schuller, J. Low Temp. Phys. **54**, 501 (1984)
12. K. Kanoda, H. Mazaki, T. Yamada, N. Hosoito, T. Shinjo, Phys. Rev. B **33**, 2052 (1986)
13. P.R. Broussard, T.H. Geballe, Phys. Rev. B **35**, 1664 (1987)
14. C. Cirillo, C. Attanasio, L. Maritato, L.V. Mercaldo, S.L. Prischepa, M. Salvato, J. Low Temp. Phys. **130**, 509 (2003)
15. R.T.W. Koperdraad, A. Lodder, Phys. Rev. B **54**, 515 (1996)
16. J. Aarts, Phys. Rev. B **56**, 8432 (1997)
17. W. Maj, J. Aarts, Phys. Rev. B **44**, 7745 (1991)
18. B.J. Yuan, J.P. Whitehead, Phys. Rev. B **47**, 3308 (1993)
19. V.N. Kushnir, A.Yu. Petrov, S.L. Prischepa, Low Temp. Phys. **25**, 948 (1999)
20. P.G. de Gennes, Rev. Mod. Phys. **36**, 225 (1964)
21. A.A. Abrikosov, *Fundamentals of the Theory of Metals* (Nauka, Moscow, 1987)
22. P.G. de Gennes, *Superconductivity in Metals and Alloys*, edited by W.A. Benjamin (Inc. New York – Amsterdam, 1966)
23. I.K. Schuller, Phys. Rev. Lett. **44**, 1597 (1980)
24. G.J. Nieuwenhuys, Adv. Phys. **24**, 515 (1975)
25. C. Cirillo, S.L. Prischepa, M. Salvato, C. Attanasio, Eur. Phys. J. B **38**, 59 (2004)